Nonlin. Processes Geophys. Discuss., 1, 1331–1363, 2014
www.nonlin-processes-geophys-discuss.net/1/1331/2014/
doi:10.5194/npgd-1-1331-2014

Nonlinear Processes in Geophysics
Discussions
Open Access

Geometric and topological approaches to significance testing in wavelet analysis

J. A. Schulte[1], C. Duffy[2], and R. G. Najjar[1]

[1]Department of Meteorology, The Pennsylvania State University, University Park, Pennsylvania, USA
[2]Department of Civil Engineering, The Pennsylvania State University, University Park, Pennsylvania, USA

Received: 11 July 2014 – Accepted: 28 July 2014 – Published: 13 August 2014

Correspondence to: J. A. Schulte (jas6367@psu.edu)

Published by Copernicus Publications on behalf of the European Geosciences Union & the American Geophysical Union.

Abstract

Geometric and topological methods are applied to significance testing in the wavelet domain. A geometric test was developed for assigning significance to pointwise significance patches in local wavelet spectra, contiguous regions of significant wavelet coefficients with respect to some noise model. This geometric significance test was found to produce results similar to an existing areawise significance test, while being more computationally flexible and efficient. The geometric significance test can be readily applied to pointwise significance patches at various pointwise significance levels in wavelet power and coherence spectra. A topological analysis of pointwise significance patches determined that holes, deficits in pointwise significance embedded in significance patches, are capable of identifying important structures, some of which are undetected by the geometric and areawise tests. The application of the new and existing significance tests to ideal time series and to the time series of the Niño 3.4 and North Atlantic Oscillation showed that the areawise and geometric tests perform similarly in ideal and geophysical settings, while the topological methods showed that the Niño 3.4 time series contains numerous phase-coherent oscillations.

1 Introduction

Time series are often complex, composed of oscillations and trends. The goal of researchers is to decide whether the embedded structures in the time series are random or meaningful. Such decisions can be made using Fourier analysis, with the assumption that the underlying time series is stationary (Jenkins and Watts, 1968). In many cases, however, the stationary assumption is not satisfied, making Fourier analysis an inappropriate tool for feature extraction. For non-stationary time series, wavelet analysis (Meyers, 1993; Torrence and Compo, 1998) can be used for decomposing a time series into both frequency and time components, allowing the extraction of transient features and dominant modes of variability. Once embedded structures in time series

NPGD
1, 1331–1363, 2014

have been identified, a natural question arises: what physical mechanisms are responsible for the detected modes of variability? Linkages between the modes of variability and possible physical mechanisms can be obtained using wavelet coherence (Grinsted et al., 2004), a bivariate tool for detecting common oscillations between two time series. Together, wavelet power and coherence analyses have proven useful in climate science (Velasco and Mendoza, 2007; Muller et al., 2008), hydrology (Zhang et al., 2006; Ozger et al., 2009; Labat, 2008, 2010), atmospheric science (Terradellas et al., 2005; Schimanke et al., 2011), and oceanography (Lee and Lwiza, 2008).

The application of wavelet analysis alone is not sufficient for feature extraction of time series; indeed, random fluctuations can produce large values of spectral power or coherence related to the underlying process (e.g., red-noise) and not necessarily the time series. In Fourier analysis, one chooses a suitable noise model and assesses the significance of features relative to some analytically or empirically derived threshold. In climate science, for example, one often compares the sample power spectrum of a time series to that of a theoretical red-noise spectrum. Statistical significance testing is also necessary in the wavelet domain. Torrence and Compo (1998) were the first to assess the significance of features in wavelet power spectra using red-noise background spectra. Grinsted et al. (2004), using Monte Carlo methods, extended significance testing to wavelet coherence using surrogate red-noise time series. The (pointwise) significance tests developed by Torrence and Compo (2010) and Grinsted et al. (2004), however, have multiple testing problems, given the large number of wavelet coefficients being tested simultaneously (Maraun and Kurths, 2004). Maraun et al. (2007) addressed these problems by sorting through pointwise significance patches based on their size and geometry, minimizing spurious results, and thus giving researchers more insight into the time series in question.

In this study, significance testing in the wavelet domain is improved through the following: (1) the development of a flexible and computationally efficient geometric test capable of minimizing spurious results from the pointwise test by associating p values to individual patches in wavelet-power and wavelet-coherence spectra; and (2) the application of topological methods that can further distinguish spurious patches from true structures that can reveal information about time series undetected by current methods. Given the deficiencies of pointwise significance testing, there is a need to improve current methods of evaluating significance of features in the wavelet domain. Moreover, the areawise test, though a substantial improvement from the pointwise test has one drawback: finding the significance level of the areawise test requires a complicated root-finding algorithm, making p values for the areawise test difficult to obtain, as it would require the repeated application of a root-finding algorithm (see Sect. 4.1 for details).

The remainder of the paper is organized as follows. A brief overview of wavelet analysis is presented in Sect. 2. In Sect. 3, the pointwise and areawise tests are discussed briefly. The development of the geometric test is presented in Sect. 4. In Sect. 5, ideas inspired by persistence homology (Edelsbrunner, 2010) are used to show that holes can distinguish important structures from trivial structures, linking the geometric and topological tests. Using ideas from Sects. 4 and 5, the application of a local geometric test is presented in Sect. 6. The new methods are applied to time series of two idealized cases, which provide important benchmarks for the methods, and to indices of two prominent climate modes, El Niño and the North Atlantic Oscillation (NAO), to illustrate, in a geophysical setting, the insights afforded by the methods.

2 Definitions

In wavelet analysis, a time series is decomposed into frequency and time components by convolving the time series with a wavelet function satisfying certain conditions. There are many different kinds of wavelet functions but the most widely used is the Morlet wavelet, a sine wave damped by a Gaussian envelope expressed as

$$\psi_0(\eta) = \pi^{-1/4} e^{i\omega_0 \eta} e^{-\frac{1}{2}\eta^2}, \tag{1}$$

where ψ_0 is the Morlet wavelet, ω_0 is the dimensionless frequency, and $\eta = s \cdot t$, where s is the wavelet scale (Torrence and Compo, 1998; Grinsted et al., 2004). The wavelet transform of a discrete time series x_n ($n = 1, \ldots, N$) is given by

$$W_n^X(s) = \sqrt{\frac{\delta t}{s}} \sum_{n'=1}^{N} x_{n'} \psi_0[(n' - n)] \frac{\delta t}{s}, \tag{2}$$

where δt is a uniform time step determined from the time series and $\left|W_n^X(s)\right|^2$ is the wavelet power of a time series at scale s and time index n (Torrence and Compo, 1998; Grinsted et al., 2004). Note that for the Morlet wavelet with $\omega_0 = 6$ the wavelet scale and the Fourier period λ are approximately equal ($\lambda = 1.03s$).

3 Existing significance testing methods

3.1 Pointwise significance testing

For climatic time series, the significance of wavelet power can be tested against a theoretical red-noise background (Torrence and Compo, 1998). Time series and wavelet power spectra for the NAO index (Hurrell et al., 1995, https://climatedataguide.ucar.edu/climate-data/hurrell-north-atlantic-oscillation-nao-index-station-based) and the Niño 3.4 index (Trenberth, 1997, http://www.cgd.ucar.edu/cas/catalog/climind/Nino_3_3.4_indices.html) are shown in Figs. 1 and 2. The wavelet power spectrum of the NAO index reveals numerous time periods of enhanced variance at an array of time scales, though no preferred timescale is evident. For the Niño 3.4 index, the wavelet power spectrum detects statistically significant variance in the 16–64 month period band for the period 1960–2010. Another interesting feature emerges: periods of reduced pointwise significance surrounded by regions of pointwise significance. These “holes” will turn out to be important structures in wavelet power spectra and are discussed thoroughly in Sect. 5.

NPGD
1, 1331–1363, 2014

3.2 Areawise significance testing

The idea behind the Maraun et al. (2007) areawise test (hereafter simply the "areawise test") is that correlations between adjacent wavelet coefficients arising from the reproducing kernel (see Appendix A) produce continuous regions of pointwise significance that resemble the reproducing kernel. For the wavelet transformation of Gaussian white noise, the correlation between wavelet coefficients at (b,a) and (b',a'), $C(b,a,b',a')$, is given by the reproducing kernel moved to time b and stretched to scale a (Maraun and Kurths, 2004; Maraun et al., 2007). Thus, for significance patches generated from random fluctuations, the typical patch area is given by the reproducing kernel. The test can be described more formally as follows: let P_{pw} be the set of all pointwise significance values and define a critical area $P_{\text{crit}}(b,a)$ as the subset of the time-scale domain for which the reproducing kernel K, dilated and translated to time b and scale a, exceeds the threshold of a critical level K_{crit}. Mathematically, $P_{\text{crit}}(b,a)$ is given by

$$P_{\text{crit}}(b,a) = \{(b',a') : K(b,a;b',a') > K_{\text{crit}}\}. \tag{3}$$

For a patch of pointwise significant values, a point inside the patch is said to be areawise significant if any reproducing kernel dilated according to the scale in question entirely fits into the patch, i.e.

$$P_{\text{aw}} = \bigcup_{P_{\text{crit}}(b,a)\subset P_{\text{pw}}} P_{\text{crit}}(b,a), \tag{4}$$

where P_{aw} is the subset of pointwise significant values consisting of additionally areawise significant wavelet coefficients. The critical area is related to significance level of the areawise test by the following equation:

$$1-\alpha_{\text{aw}} = 1-\left\langle \frac{A_{\text{aw}}}{A_{\text{pw}}} \right\rangle, \tag{5}$$

where $1-\alpha_{\text{aw}}$ is the significance level of the areawise test, A_{aw} is the area of the areawise significance patch, A_{pw} is the area of the pointwise significance patch, and

NPGD
1, 1331–1363, 2014

$\langle \frac{A_{aw}}{A_{pw}} \rangle$ is the average ratio between the areas of areawise significant patches and the pointwise significance patches. It turns out that the calculation of α_{aw} is non-trivial, involving a root-finding algorithm that solves the equation $f(P_{crit}) - \alpha_{aw} = 0$ (see Sect. 4).

To illustrate the importance of the areawise significance test, the test was applied to the wavelet power spectra of the NAO and Niño 3.4 index time series (Figs. 1 and 2). Numerous pointwise significance patches in the Niño 3.4 wavelet power spectrum were found to contain areawise significant subsets, suggesting that these patches were less likely to be an artifact of multiple testing. The wavelet power spectrum of the NAO index also contained pointwise significance patches with areawise significant subsets, all of which were at high frequencies.

4 Geometric significance testing

4.1 Development

The development of a geometric significance test will require ideas from basic geometry and set theory. To begin, each patch in the wavelet domain will be considered a polygon with a finite set of vertices $p_i = (t_i, s_i)$, where t_i is a time index and s_i is a scale index whose maximum is

$$J = \delta j^{-1} \log_2 \left(\frac{N \delta t}{s_{min}} \right), \tag{6}$$

where N is the length of the time series, δt is a time step, and s_{min} is the smallest resolvable scale (Torrence and Compo, 1998). Note that the quantity δj depends on the wavelet function, being approximately equal to 0.5 for the Morlet wavelet. Using the scale index instead of the actual scale value will allow a simpler computation of area; indeed, in this coordinate system the width of significance patches does not depend on scale, whereas using actual scale values would result in a coordinate system in which patches widen with increasing scale. It is worth noting that not all patches are closed in

NPGD
1, 1331–1363, 2014

the sense that some are located near the edges of the wavelet domain. To remedy this problem, semi-enclosed patches are artificially closed by connecting the two vertices located on the boundary of the wavelet domain with a line segment.

Perhaps the most fundamental property of a pointwise significance patch is its area, which can be calculated using the following special case of Green's Theorem:

$$A = \frac{1}{2}\left|\sum_{i=0}^{n-1}(t_i s_{i+1} - t_{i+1}s_i)\right|, \tag{7}$$

where $s_0 = s_n$ and $t_0 = t_n$. For significance patches containing holes, the total area of the holes is subtracted from the area the significance patch would have it did not contain the holes.

What will be of particular interest is the normalized area of a significance patch, not its absolute area. To compute the normalized area, the centroid of a significance patch will need to be calculated using the following formulas:

$$C_\mathrm{t} = \frac{1}{6A}\sum_{i=0}^{n-1}(t_i + s_{i+1})(t_i s_{i+1} - t_{i+1}s_i) \tag{8}$$

and

$$C_\mathrm{s} = \frac{1}{6A}\sum_{i=0}^{n-1}(s_i + t_{i+1})(t_i s_{i+1} - t_{i+1}s_i), \tag{9}$$

where C_t and C_s are the time and scale coordinates, respectively, of the centroid. Recall that the centroid is the area-weighted location of a polygon. If A_R is the area of the reproducing kernel dilated or contracted (at a certain critical level) to $(C_\mathrm{t}, C_\mathrm{s})$, then the normalized area of a significance patch is given by

$$A_n = \frac{A}{A_\mathrm{R}}, \tag{10}$$

NPGD
1, 1331–1363, 2014

Geometric and topological approaches to significance testing in wavelet analysis

J. A. Schulte et al.

and allows one to compare sizes of significance patches across all scales simultaneously. Two idealized pointwise significance patches with equal normalized area are shown in Fig. 3a and b.

The quantity that will be of importance in the development of the geometric significance test is convexity, which describes the degree to which a polygon or point set lacks concavities. The reason for including convexity is illustrated by considering the two significance patches shown Fig. 3, which have equal values of A_n but different geometries: one is convex (i.e., has no concavities, Fig. 3a) and the other is not convex (Fig. 3b). Suppose that an areawise test was performed on the two patches. The reproducing kernel is capable of fitting entirely inside the convex patch but is unable to fit inside the non-convex patch as a result of the concavity. Thus, although having equal normalized area, the two patches differ in their significance, where the difference in significance is related to their geometry. It will therefore be necessary to include convexity in the geometric test, as patches of equal normalized area need to be distinguished when evaluating their significance.

Rigorously, convexity is defined as follows: Let x and y be any two points in a set Z; then the set Z is convex if for all t the line segment

$$[x,y] = \{tx + (1-t)y : 0 \leq t \leq 1\} \tag{11}$$

is in Z (Ziegler, 1995). Equivalently, a set is convex if it contains any line segment joining any pair of points in Z. Under this definition, for example, patches with thin bridges as described by Maraun et al. (2007) are not convex.

To quantify convexity, another idea from set theory, the convex hull, will be needed, which for a point set Z is defined as the intersection of all convex sets containing Z (Ziegler, 1995). In other words, it is the smallest convex set containing Z constructed from the intersection of all convex sets containing Z. Mathematically, the convex hull of a point set Z is expressed as

$$\text{conv}\,(Z) = \bigcap \{Z' \subseteq R^2 : Z \subseteq Z', Z' \text{ convex }\}. \tag{12}$$

NPGD
1, 1331–1363, 2014

In practical applications, the convex hull of a set can be easily computed using existing algorithms (Barber et al., 1996). It is noted that all holes are ignored in the computation of the convex hull.

A metric for convexity will now be defined using the area of a significance patch together with the area of its convex hull as follows: if A_k is the area of the convex hull of a significance patch whose area is A, then the convexity is

$$\mathcal{C} = \frac{A}{A_k}, \tag{13}$$

where $0 \leq \mathcal{C} \leq 1$. High values of $\mathcal{C}$ correspond to significance patches with relatively small concavities, whereas small values of $\mathcal{C}$ correspond to patches with relatively large concavities, as in the case of significance patches with thin bridges.

The convexity along with the convex hulls of the two idealized patches is shown in Fig. 3. For the non-convex patch, the area of the convex hull is larger than the area of the patch itself, indicating the presence of concavities. To construct a formal statistical test, both the normalized area and convexity will be important. A simple quantity combining both the area and geometry of a patch is the following:

$$\chi = \mathcal{C}A_n, \tag{14}$$

where larger values of χ indicate more significant patches. The index χ for the two idealized patches shown Fig. 3 is 2.8 for the convex patch and 2.1 for the non-convex patch, the difference arising from the convexity.

The idea of the geometric significance test is to generate a null distribution of χ and use the null distribution to compute the significance of patches in the wavelet domain. In climate science, a suitable null hypothesis is red-noise so that χ will be computed for a large ensemble of patches generated from red-noise processes. Using the null distribution of χ, one can assign to each patch in the wavelet domain a probability p that the patch was not generated from a random stochastic fluctuation. The application of the geometric significance test to the two idealized patches (see Fig. 3) would

NPGD
1, 1331–1363, 2014

result in the convex patch having greater significance despite the fact that the patches have equal normalized area. Therefore, χ can correctly distinguish the significance of patches based only on area and convexity.

The calculation of the geometric significance level $1-\alpha_g$, unlike the calculation of $1-\alpha_{aw}$, is straightforward: for the areawise test one needs to compute α_{aw} as a function of P_{crit}, whereas for the geometric test α_g is no longer a function P_{crit}. Moreover, the estimation of P_{crit} involves a root-finding algorithm that solves the equation $f(P_{crit})-\alpha_{aw}=0$, where $f(P_{crit})$ is estimated using Monte Carlo simulations. Thus, the application of the areawise test to pointwise significance patches for m different values of α_{aw} would require m Monte Carlo ensembles, making p values for the test difficult to obtain. For the geometric test, only a single Monte Carlo ensemble is needed, as a single choice of P_{crit} is needed to generate a null distribution, from which any desired value of α_g can be obtained. In fact, while the choice of P_{crit} impacts the mean value of the null distribution, the geometric significance of a significance patch is left unchanged, as the significance is relative to a distribution of χ under some noise model (Appendix B).

The elimination of the P_{crit} dependence from the calculation of the geometric significance level allows the geometric test to be readily performed on patches of various pointwise significance levels. For the areawise test, a new P_{crit} must be estimated for each pointwise significance level since A_{pw}, on average, will change depending on if the pointwise significance level $1-\alpha_p$ is increased (patches shrink) or is decreased (patches grow). For the geometric test, there is no need to find a new P_{crit} – simply compute a new null distribution based solely on the information of the pointwise significance patches at some pointwise significance level $1-\alpha_p$.

Another advantage of eliminating the P_{crit} dependence is that the geometric test can be readily applied to wavelet coherence, partial wavelet coherence (Ng, 2012), multiple wavelet coherence, and cross-wavelet spectra. The application of the geometric test to significance patches in the aforementioned wavelet spectra only requires a single Monte Carlo ensemble to generate a null distribution, eliminating the calculation of a new P_{crit} for each wavelet spectra and for each value of α_g. For the areawise test,

NPGD
1, 1331–1363, 2014

a new P_{crit} must be estimated for each value of α_{aw} and for each wavelet spectra, making the areawise test difficult to implement in practical applications.

It may happen that a pointwise significance patch is so large that individual oscillations embedded in the patch cannot be detected by the geometric test. However, there are two solutions to this localization problem: the first solution is to increase the significance level of the pointwise test, allowing large patches to separate, and then perform the geometric test on the smaller patches. The second solution is to examine other properties of significance patches that may indicate the presence of multiple periodicities that form large significance patches from the merging of several smaller patches. The second solution will be addressed thoroughly in Sect. 5.

4.2 Comparisons with the areawise test

With a formal geometric significance test now developed, it is useful to compare the areawise and geometric significance tests, where comparisons will be made using an empirically derived quantity. Let N_{sig} be the number of pointwise significance patches in a given wavelet power spectrum, N_a the number of patches containing an areawise significant region, N_g the number of geometrically significance patches, and N_{ag} the number patches that are both geometrically significant and that contain areawise significant regions. The quantity

$$I_{sim} = \frac{N_{sig} - N_a - N_g + 2N_{ag}}{N_{sig}} \quad (15)$$

then measures the similarity between the two tests. The interpretation of I_{sim} is as follows: if $I_{sim} = 1$ then all patches containing areawise significant regions are also geometrically significant and all patches which do not contain areawise significant regions are also not geometrically significant. On the other hand, for values of I_{sim} less than 1 some patches containing areawise significant regions may not be geometrically significant, with the converse also being true.

NPGD
1, 1331–1363, 2014

To better compare the similarity between the two tests, distributions of I_{sim} were constructed by generating a large number of synthetic wavelet power spectra of red-noise processes with fixed autocorrelation coefficients equal to 0.5 and computing I_{sim} for each of the synthetic wavelet power spectra. The results are shown Fig. 4a. With a mean value of 0.90, a strong agreement was found between the areawise and geometric tests, differences arising from the fact that the areawise test is a local test, finding significant regions within patches, whereas the geometric test assigns a significance value to entire patches. Since I_{sim} was often less than 1.0, some patches containing areawise-significant regions were not found to be geometrically significant, and, conversely, some patches were geometrically significant without containing areawise-significant regions.

The quantity $r_{neg} = N_g/N_a$, which measures the ratio of false positive results between both tests, was also computed (Fig. 4b). The mean value of r_{neg} was found to be 1.1 and the median value was found to be 1.0, indicating that both tests, on average, falsely deemed the same number of pointwise significance patches as significant for a given wavelet power spectrum, consistent with the fact that the significance levels of both tests were set to 0.9. However, the distribution shown in Fig. 4b was found to be positively skewed with skewness equal to 2.8, implying that, in many cases, the geometric test results in fewer false–positive results.

4.3 Geometric significance testing of climatic data

For climatic time series, significance is often tested against a red-noise background and therefore it is reasonable to expect that the areawise and geometric tests behave similarly when applied to climatic time series. As such, the areawise and geometric tests were applied to the NAO and Niño 3.4 time series. For the wavelet power spectrum of the NAO index time series (see Fig. 1), geometrically significant patches were identified, one of which was also areawise significant. The geometrically significant patches were mainly located at high frequencies, suggesting enhanced, although transient, seasonal variability. The wavelet power spectrum of the Niño 3.4 index (see Fig. 2) was

NPGD
1, 1331–1363, 2014

Geometric and topological approaches to significance testing in wavelet analysis

J. A. Schulte et al.

Title Page
Abstract Introduction
Conclusions References
Tables Figures
◀◀ ▶▶
◀ ▶
Back Close
Full Screen / Esc
Printer-friendly Version
Interactive Discussion

found to contain two geometrically significant patches, both of which were located in the period band of 16–64 months after 1950. The significance patch centered at 1985 and at a period of 32 months, however, is so large that individual oscillations could not be identified. To remedy the problem, the geometric significance was applied to 99 % ($\alpha_p = 0.01$) pointwise significance patches, resulting in five significance patches being detected, with many of the patches containing areawise-significant regions also found to be geometrically significant. Both tests deemed the significance patches centered at periods less than 12 months as insignificant.

5 Topological significance testing

5.1 Topological significance testing of ideal time series

Topology is a branch of mathematics concerned with properties of spaces that remain unchanged after continuous deformations. So far only geometric aspects of significance patches have been discussed. Area of a significance patch, as an example, is a geometric property in the sense that stretching the patch in both the scale and time direction would increase its area. There are properties, however, that would be unaffected by stretching the significance patch. As a motivating example, consider the wavelet power spectrum of the Niño 3.4 index shown in Fig. 2, where there is a hole or region of significance deficit located within a significance patch. This feature is topological, as the hole would remain under a continuous deformation such as stretching.

To begin the topological analysis, the topology of time series with known structures will be analyzed. Given the importance of red-noise processes in the spectral analysis of climatic time series, the topology of patches generated from red-noise processes is first considered to determine if pointwise significance patches can be distinguished from those generated from red-noise processes solely based on their topology. To answer this question, a large ensemble of pointwise significance patches arising from red-noise processes was generated and the number of holes (denoted by N_h hereafter) at a finite set of pointwise significance levels was computed (Fig. 5). It was found that N_h is not a random function of the pointwise significance level, as indicated by the 95 % confidence bounds. Most importantly, for pointwise significance levels greater than 90 %, few patches contained holes, suggesting that holes are an uncommon feature of significance patches generated from red-noise processes (Table 1) and therefore can be used to distinguish spurious patches from important structures. A simple algorithm for assessing the significance of holes is therefore developed. To find the significance of holes, plot the centroids of holes at a finite set of pointwise significance levels and project the centroids onto the wavelet domain, resulting in a topological wavelet diagram. In accordance with Fig. 5, regions in the wavelet domain where holes exist above the 80 % pointwise significance level will be considered regions with significant topological features.

With a method for assessing the significance of holes, it is reasonable to analyze different ideal time series, both linear and nonlinear, to determine what types of time series produce holes in significance patches. Perhaps the simplest case is a single sinusoid with additive white noise (not shown). In this case, no evidence was found that a single sine wave is capable of generating holes in 95 % significance patches, implying holes arise from a much richer structure embedded in time series. Thus, two more complex cases are considered.

To derive the Case I time series, first consider the nonlinear system

$$X_{out}(t) = bX_{in}(t) + \gamma X_{in}^2(t), \tag{16}$$

where $X_{in}(t)$ is the input into the system, $X_{out}(t)$ is the output of the system, b is a linear coefficient, and γ is a nonlinear coefficient. The output from this system will be quadratically phased coupled (King, 1996), where quadratic phase coupling indicates that for frequencies f_1, f_2, and f_3 and corresponding phases ϕ_1, ϕ_2, and ϕ_3 the sum rules $f_1 + f_2 = f_3$ and $\phi_1 + \phi_2 = \phi_3$ are satisfied. In Case 1, $X_{in} = \cos 2\pi f t$ so that

$$X_{out}(t) = \frac{\gamma}{2} + b\cos 2\pi f t + \frac{\gamma}{2}\cos 4\pi f t, \tag{17}$$

NPGD
1, 1331–1363, 2014

Geometric and topological approaches to significance testing in wavelet analysis

J. A. Schulte et al.

indicating that the output contains an additional frequency component at the harmonic $2f$ (harmonic generation) and the mean value of the output has shifted (rectification) with respect to the input. Figure 6a and b shows the time series of X_{out} with the corresponding wavelet power spectrum for the case when $f = 1/64 = 1/\lambda_1$, $b = 1$, $\phi_1 = \pi/2$, $\phi_2 = \pi/3$, and $\gamma = 0.25$ (arbitrary units) and with Gaussian white noise added to the output. The wavelet power spectrum of the output contains numerous pointwise significant patches, all of which are spurious except for the one at $\lambda_1 = 64$. The areawise and geometric test correctly identified the pointwise significance patch at $\lambda_1 = 64$ to be significant but deemed two spurious patches as significant at high frequencies. Note that the pointwise significance test was unable to detect the harmonic with period $\lambda_2 = 32$. It should be noted, however, that if the parameter γ were increased, the oscillation with period $\lambda_2 = 32$ would become more prominent. In fact, it was found that for larger values of γ the areawise and geometric tests perform better (not shown), correctly identifying the oscillation with period $\lambda_2 = 32$, with the result also depending on the noise level. Case 1 thus only serves as an illustrative example of a situation that may arise when a wavelet analysis is applied to a geophysical (often noisy) time series.

To extract more information from the wavelet power spectrum, the centroids of holes were plotted as a function of the pointwise significance level (Fig. 6c). The top panel shows that holes only existed at low pointwise significance levels. Therefore, not all nonlinear time series can generate holes at high pointwise significance levels, suggesting that the relative difference between the primary frequency components or the resulting frequency combinations is important, as discussed below.

Case 2 is the quadratically phase-coupled time series

$$X(t) = \cos(2\pi f_1 t + \phi_1) + \cos(2\pi f_2 t + \phi_2) + \gamma \cos[2\pi(f_1 + f_2)t + \phi_1 + \phi_2], \quad (18)$$

which consists of three frequency components: $f_1 = 1/20 = 1/\lambda_1$, $f_2 = 1/30 = 1/\lambda_2$, and $f_1 + f_2 = 1/12 = 1/\lambda_3$, and γ is assumed to be 0.5. Unlike the wavelet power spectrum of Case 1, holes have appeared in 95 % pointwise significance patches between periods $\lambda_1 = 20$ and $\lambda_2 = 30$ (Fig. 7b). Moreover, the pointwise significance patch containing the hole (labeled P_1) was found to be geometrically significant and was found to contain an areawise-significant subset in the lower portion of the patch. It is worth noting that the areawise test failed to detect a significant periodicity at $\lambda_1 = 20$ despite the fact that it is known to exist by construction. In particular, the upper portion of the pointwise significance patch P_1 was not found to be significant. Figure 7c shows that a few holes existed at large pointwise significant levels ($\geq 80\,\%$), though only one was found at the 95 % pointwise significance level. However, according to Fig. 5, the holes existing at the 80 % pointwise level may indicate the presence of significant features. For example, the geometric and areawise tests deemed the patch labeled P_2 in Fig. 7b as insignificant, though the topology of the patch at the 80 % pointwise significant level suggests the existence of a significant feature. Indeed, the proximity of the significant holes to the pointwise significance patches labeled P_2 and P_3 suggests that those patches are significant (see Sect. 5 for a detailed discussion). The topology of patches at an array of pointwise significance levels can therefore uncover information about time series that may have gone undetected using the pointwise, geometric, and areawise tests.

Like with Case 1, the Case 2 results also depend on γ, the amplitudes of the cosines, and the noise level, with holes, after further investigation (not shown), being more prominent in low-noise situations. Moreover, both the areawise and geometric tests were found to better identify the correct oscillations when the noise level was reduced. Case 2 illustrates the insights gained when considering the topological properties of significance patches.

Though both wavelet power spectra represent a time series generated from a quadratic nonlinearity, the nonlinear interaction in Case 2 contained oscillations with nearby frequency components, allowing the formation of holes, whereas for Case 1 no significant holes appeared in the wavelet power spectrum. Since the presence of holes depends on the relative location of two oscillations in the frequency domain, it is reasonable to suspect that there exists a critical frequency difference Δf_{crit}, which measures the maximum frequency difference for which holes will appear in the wavelet

NPGD
1, 1331–1363, 2014

Geometric and topological approaches to significance testing in wavelet analysis

J. A. Schulte et al.

power spectrum. An empirically derived Δf_{crit} was determined by generating a large ensemble of time series of the form

$$x(t) = \cos 2\pi f_1 t + \cos 2\pi f_2 t + w(t), \tag{19}$$

where $f_2 > f_1 > 0$ were generated at random, $w(t)$ is additive white noise, and all the time series were of a fixed length. The signal-to-noise ratio was fixed. Figure 8 shows the mean value of N_{h} as a function of $\Delta r = (f_2 - f_1)/f_2$, the relative fractional change. For $\Delta r = 0.5$, holes never appeared, whereas for $\Delta r = 0.3$ holes appeared frequently. There is therefore a preferred frequency combination for which holes are more likely to appear. It was estimated that the upper critical value of Δr is $\Delta r_{\text{crit}} = 0.45$. Using the definition of Δr, one can write $\Delta f_{\text{crit}} = 0.45 f_2$ and therefore the critical frequency difference is a function of f_2.

The empirical results shown in Fig. 8 have theoretical implications. Suppose that the frequency components of the two oscillations were such that $f_2 = 2f_1$. In this case, $\Delta r = 0.5$ and therefore holes will almost never appear in 95 % pointwise significance patches, making the detection of quadratic phase coupling using topological methods more difficult in the case of self-interactions. More generally, suppose that a single sinusoid $X_{\text{in}}(t) = \cos 2\pi f t$ is passed through the nonlinear system

$$X_{\text{out}}(t) = bX_{\text{in}}(t) + \gamma X_{\text{in}}^{2n}(t) \tag{20}$$

where, after using the power-reduction for a cosine (Beyer, 1987), the output is given by

$$X_{\text{out}}(t) = b\cos 2\pi f t + \frac{\gamma}{2^{2n}}\binom{2n}{n} + \frac{\gamma}{2^{2n-1}}\sum_{k=0}^{n-1}\binom{2n}{k}\cos 4\pi f(n-k)t, \tag{21}$$

where n is a positive integer and $\binom{n}{q}$ is a binomial coefficient. For the cosines in the summation, the frequency difference between any two cosines is

$$\Delta f = 4\pi f(n-p) - 4\pi f(n-m) = 4\pi f(m-p), \tag{22}$$

NPGD
1, 1331–1363, 2014

where $0 \leq p < m \leq n-1$. Thus,

$$\Delta r = (f_2 - f_1)/f_2 = \frac{4\pi f(m-p)}{4\pi f(n-p)} = \frac{m-p}{n-p}. \tag{23}$$

Using the fact that holes mostly appear between oscillation pairs with $\Delta r < 0.45$, one can show that for large n more holes are able to appear in wavelet power spectra. In this case, holes can form in the wavelet spectrum since, for example, if $m = 5$ and $p = 6$ with $n = 10$ the inequality $\Delta r < 0.45$ will be satisfied. The result also holds if the order of the nonlinear interaction was odd and if the cosine function $X_{\text{in}}(t)$ was replaced by a sine function. For an odd order nonlinear interaction, however, $\Delta r = (2m-2p)/(2n+1-2p)$, where $0 \leq p < m \leq n$.

5.2 Topological significance testing of climatic time series

With a better understanding of the origins of holes contained in significance patches, the wavelet power spectra shown in Figs. 1 and 2 are now analyzed more closely. The wavelet topological diagram (Fig. 9a) corresponding to the wavelet power spectrum of the NAO is less interesting, containing few holes at high pointwise significance levels. The topological wavelet diagram corresponding to the wavelet power spectrum of the Niño 3.4 index, on the other hand, shows the existence of numerous holes at high pointwise significance levels, indicating that these patches are significant features (see Table 1). Moreover, the discussion in Sect. 5.1 suggests that phase-coherent oscillations were likely present in the Niño 3.4 time series.

6 Summary

A geometric significance test was developed for more rigorously assessing the significance of features in the wavelet domain. The geometric test, although related to the existing areawise test, was found to be more flexible in the sense that p values could

NPGD
1, 1331–1363, 2014

be readily calculated, involving a single Monte Carlo ensemble. On the other hand, the geometric test had the disadvantage of being less local than the areawise test. The topology of significant patches was also analyzed. Holes in significant patches, a topological notion, were capable of distinguishing spurious patches from true structures. The holes were identified as arising from phase-coherent oscillations with nearby frequency components and may indicate the existence of a nonlinear interaction. The new methods introduced in this paper were applied to NAO and Niño 3.4 indices, two well-known but contrasting time series. The methods developed in this paper will give researchers the tools needed for a better understanding of features found in wavelet power spectra, while also minimizing spurious results ubiquitous in wavelet spectra.

Appendix A

Let $F(a,t)$ be the continuous wavelet transform of a function $f(t)$ such that

$$F(a,t) = \iint K(a,t;a',t'')F(a',t'')\mathrm{d}a'\mathrm{d}t''. \tag{A1}$$

Then the reproducing kernel is given by

$$K = \frac{1}{C_\psi \sqrt{aa'^{5/2}}} \int \left[\psi\left(\frac{t'-t''}{a'}\right) \psi^*\left(\frac{t-t'}{a}\right) \right] \mathrm{d}t', \tag{A2}$$

where

$$C_\psi = \int_0^\infty \frac{|\Psi(\omega)|^2}{\omega} \mathrm{d}\omega < \infty, \tag{A3}$$

$\Psi(\omega)$ is the Fourier transform of ψ, and ψ^* denotes the complex conjugate. The reproducing kernel captures the structure of wavelet coefficients whereby the wavelet coefficient at any point contains information about a nearby wavelet coefficient weighted by K (Tropea, 2007).

NPGD
1, 1331–1363, 2014

Appendix B

Let $\chi_{\text{patch}}(C_t, C_s)$ be the test statistic associated with a significance patch whose centroid is (C_t, C_s) and let χ_{α_g} be the value of the test statistic corresponding to the $1-\alpha_g$ significance level of the geometric test. Writing

$$\chi_{\alpha_g} = \frac{(CA)_{\alpha_g}}{A_R} \tag{B1}$$

and

$$\chi_{\text{patch}}(C_t, C_s) = \frac{(CA)_{\text{patch}}}{A_R}, \tag{B2}$$

it follows that

$$\frac{\chi_{\text{patch}}(C_t, C_s)}{\chi_{\alpha_g}} = \frac{(CA)_{\text{patch}}}{(CA)_{\alpha_g}}, \tag{B3}$$

where $(CA)_{\text{patch}}$ is the product CA corresponding to the significance patch and $(CA)_{\alpha_g}$ is the product corresponding to the $1-\alpha_g$ significance level. Since Eq. (B3) no longer contains A_R, the relationship between $\chi_{\text{patch}}(C_t, C_s)$ and χ_{α_g} no longer depends on P_{crit}.

References

Barber, C. B., Dobkin, D. P., and Huhdanpaa, H.: Quickhull algorithm for convex hulls, ACM T. Math. Software, 22, 469–483, 1996.

Beyer, W. H.: CRC Standard Mathematical Tables, 28th Edn., CRC Press, Boca Raton, Florida, 674 pp., 1987.

Edelsbrunner, H. and Harer, J.: Persistent homology – a survey, Contemp. Math., 12, 1–26, 2010.

Grinsted, A., Moore, J. C., and Jevrejeva, S.: Application of the cross wavelet transform and wavelet coherence to geophysical time series, Nonlin. Processes Geophys., 11, 561–566, doi:10.5194/npg-11-561-2004, 2004.

Hurrell, J. W., Kushnir, Y., Ottersen, G., and Visbeck, M. (Eds.): The North Atlantic Oscillation: Climatic Significance and Environmental Impact, Geophys. Monogr. Ser., 134, American Geophysical Union, Washington, DC, 279 pp., 2003.

Jenkins, G. W. and Watts, D. G.: Spectral Analysis and its Applications, Holden-Day, San Francisco, California, 541 pp., 1968.

King, T.: Quantifying nonlinearity and geometry in time series of climate, Quaternary Sci. Rev., 15, 247–266, 1996.

Labat, D.: Wavelet analysis of the annual discharge records of the world's largest rivers, Adv. Water Resour., 31, 109–117, 2008.

Labat, D.: Cross wavelet analyses of annual continental freshwater discharge and selected climate indices, J. Hydrol., 385, 269–278, 2010.

Lee, Y. J. and Lwiza, K. M. M.: Factors driving bottom salinity variability in the Chesapeake Bay, Cont. Shelf Res., 28, 1352–1362, 2008.

Maraun, D. and Kurths, J.: Cross wavelet analysis: significance testing and pitfalls, Nonlin. Processes Geophys., 11, 505–514, doi:10.5194/npg-11-505-2004, 2004.

Maraun, D., Kurths, J., and Holschneider, M.: Nonstationary Gaussian processes in wavelet domain: synthesis, estimation, and significance testing, Phys. Rev. E, 75, 016707, doi:10.1103/PhysRevE.75.016707, 2007.

Meyers, S. D., Kelly, B. G., and O'Brien, J. J.: An introduction to wavelet analysis in oceanography and meteorology: with application to the dispersion of Yanai waves. Mon. Weather Rev., 121, 2858–2866, 1993.

Müller, W. A., Frankignoul, C., and Chouaib, N.: Observed decadal Tropical Pacific–North Atlantic teleconnections, Geophys. Res. Lett., 35, L24810, doi:10.1029/2008GL035901, 2008.

Ng, E. K. W. and Chan, J. C. L.: Geophysical applications of partial wavelet coherence and multiple wavelet coherence, J. Atmos. Ocean. Tech., 29, 1845–1853, 2012.

Özger, M., Mishra, A. K., and Singh, V. P.: Low frequency drought variability associated with climate indices, J. Hydrol., 364, 152–162, 2009.

Paluš, M. and Novotná, D.: Quasi-biennial oscillations extracted from the monthly NAO index and temperature records are phase-synchronized, Nonlin. Processes Geophys., 13, 287–296, doi:10.5194/npg-13-287-2006, 2006.

NPGD
1, 1331–1363, 2014

Schimanke, S., Körper, J., Spangehl, T., and Cubasch, U.: Multi-decadal variability of sudden stratospheric warmings in an AOGCM, Geophys. Res. Lett., 38, L01801, doi:10.1029/2010GL045756, 2011.

Terradellas, E., Soler, M. R., Ferreres, E., and Bravo, M.: Analysis of oscillations in the stable atmospheric boundary layer using wavelet methods, Bound.-Lay. Meteorol., 114, 489–518, 2005.

Torrence, C. and Compo, G. P.: A practical guide to wavelet analysis, B. Am. Meteorol. Soc., 79, 61–78, 1998.

Trenberth, K. E.: The definition of El Niño, B. Am. Meteorol. Soc., 78, 2771–2777, 1997.

Tropea, C., Yarin, A. L., and Foss, J. F. (Eds.): Springer Handbook of Experimental Fluid Mechanics, Springer, Berlin, Germany, 1557 pp., 2007.

Velasco, V. M. and Mendoza, B.: Assessing the relationship between solar activity and some large scale climatic phenomena, Adv. Space Res., 42, 866–878, 2008.

Zhang, Q., Xu, C., Jiang, T., and Wu, Y.: Possible influence of ENSO on annual maximum streamflow of the Yangtze River, China, J. Hydrol., 333, 265–274, 2007.

Ziegler, G. M.: Lectures On Polytopes, Graduate Texts in Mathematics, 152, Springer, New York, 370 pp., 1995.

NPGD
1, 1331–1363, 2014

Table 1. Fraction of pointwise significance patches containing holes as a function of the pointwise significance level calculated from an ensemble of 200 000 significance patches generated from red-noise processes with fixed autocorrelation coefficients equal to 0.5.

Significance level (%)	Fraction
85	1.0×10^{-2}
90	2.0×10^{-3}
95	3.4×10^{-4}
99	0

NPGD
1, 1331–1363, 2014

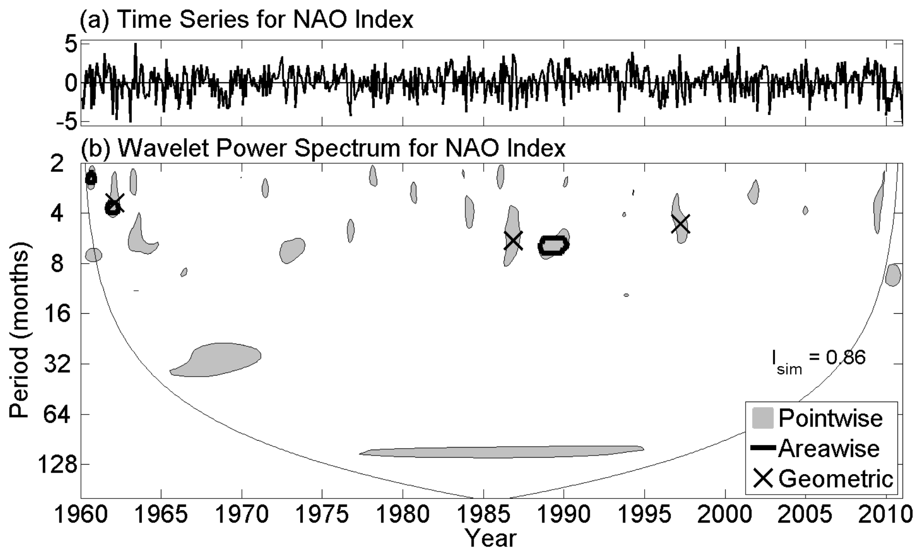

Figure 1. (a) The NAO index from 1960–2010. **(b)** Normalized wavelet power spectrum of the NAO Index mean monthly values. Gray shading are 95 % pointwise significance patches and black contours are the 90 % areawise significant subsets. Crosses indicate those patches which are geometrically significant at the 90 % level. Thin black line represents the cone of influence.

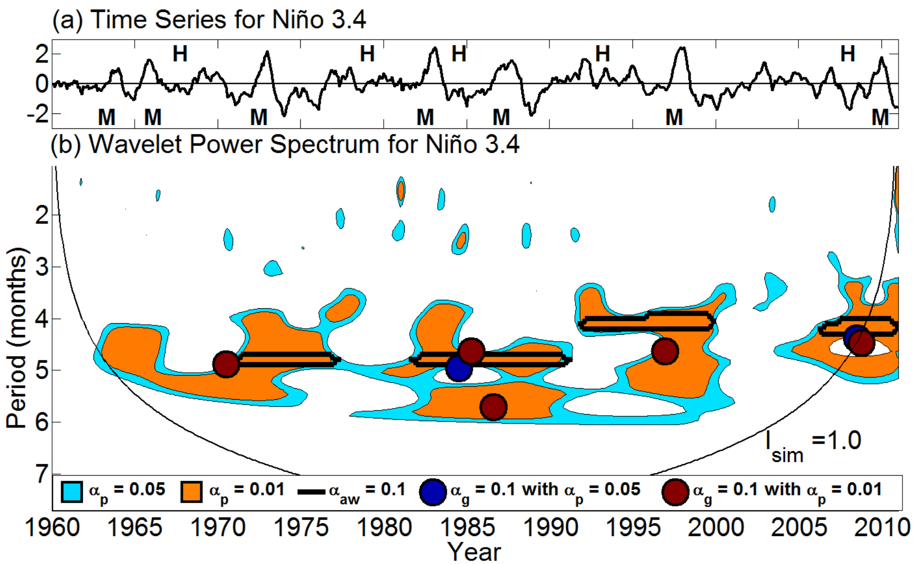

Figure 2. (a) The mean monthly Niño 3.4 index anomalies from 1960–2012. Points labeled *M* indicate points where the merging process occurred and points labeled *H* indicate points where a hole was formed (see Sect. 5.2 for details). **(b)** The normalized wavelet power spectrum of the Niño 3.4 index from 1960–2010. Orange shading are 95 % pointwise significance patches, blue shading are 99 % pointwise significance patches, and the black contours are the 90 % areawise-significant subsets of the 95 % pointwise significance patches. Blue dots indicate the centroids of those 95 % pointwise significance patches that are geometrically significant at the 90 % level and the red dots indicate the centroids of those 99 % pointwise significance patches that are 90 % geometrically significant. Thin black line represents the cone of influence. I_{sim} is reported for the case when $\alpha_{aw} = 0.1$, $\alpha_g = 0.1$, and $\alpha_p = 0.05$.

NPGD
1, 1331–1363, 2014

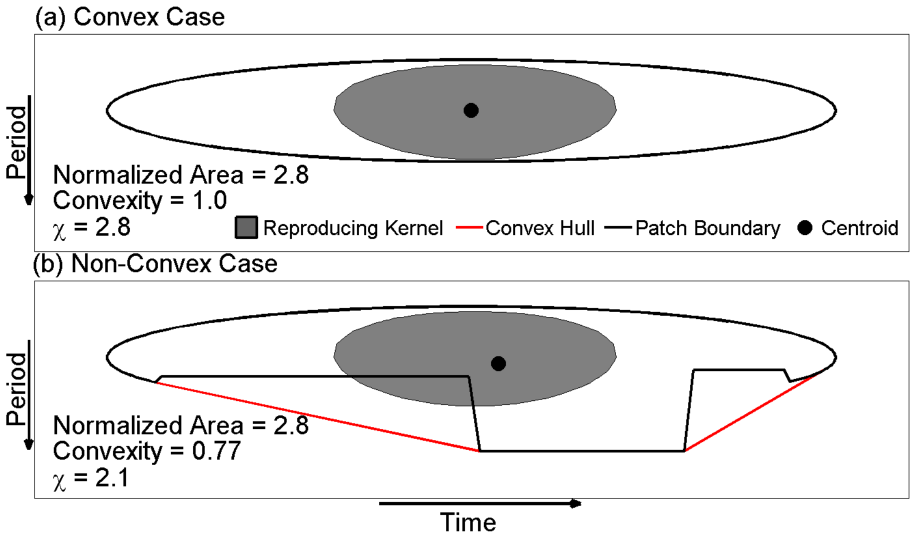

Figure 3. (a) An idealized convex pointwise significance patch whose boundary is indicated by the black contour and whose centroid is indicated by the black dot. The reproducing kernel indicated by gray shading lies entirely inside the patch. The convexity, normalized area, and χ are displayed on the bottom left corner. **(b)** Same as **(a)** except the area of the convex hull (red curve) is not equal to the area of the patch and the reproducing kernel is unable to fit entirely inside the patch.

NPGD
1, 1331–1363, 2014

Geometric and topological approaches to significance testing in wavelet analysis

J. A. Schulte et al.

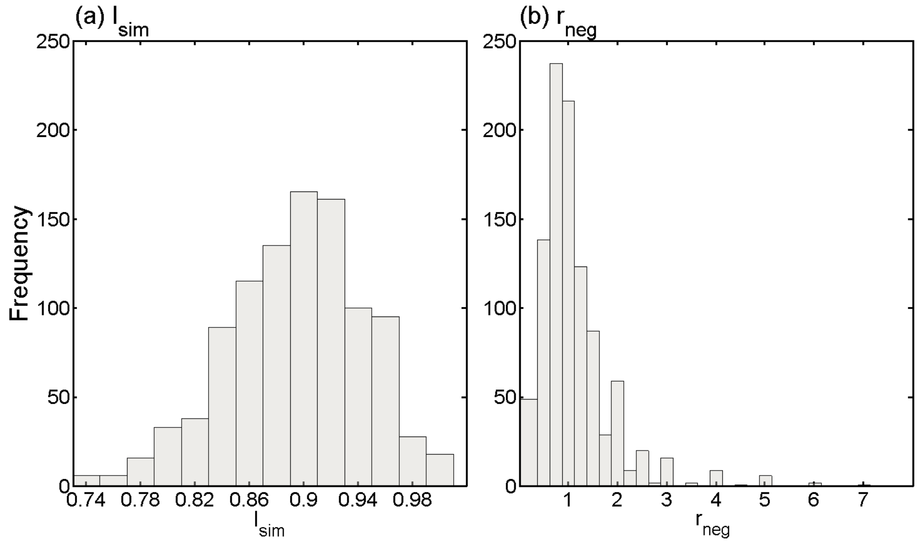

Figure 4. (a) Histogram of the similarity index between the geometric and areawise tests. The distribution was obtained by generating 1000 random wavelet spectra of red-noise processes with fixed autocorrelation coefficients equal to 0.5 and computing the similarity index for each of the 1000 synthetic wavelet spectra. The 90 % significance level was used for both the areawise and geometric tests. **(b)** Same as **(a)** except for the ratio between the false positive results of the geometric and areawise tests.

NPGD
1, 1331–1363, 2014

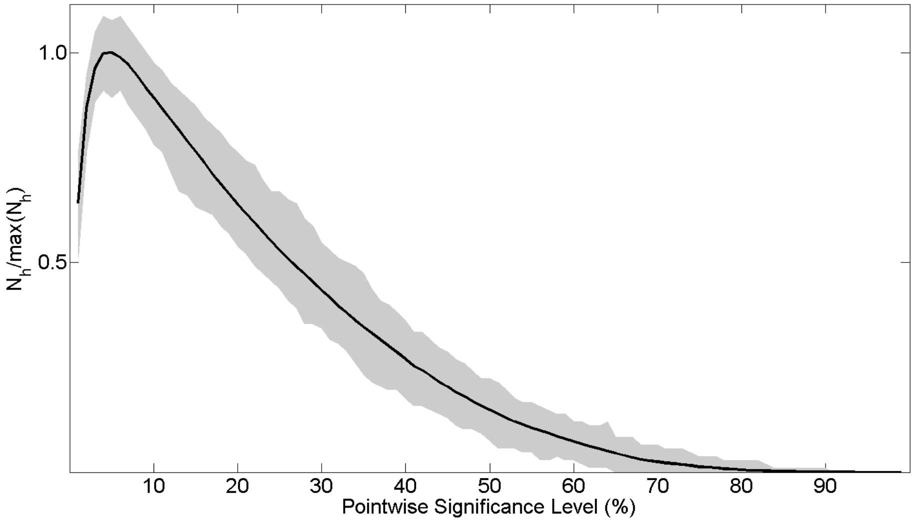

Figure 5. Normalized mean number of holes as a function of pointwise significance level. The number of holes was calculated by generating 10 000 synthetic wavelet power spectra of red-noise processes with fixed autocorrelation coefficients of 0.5 and computing the number of holes Gray shading represents the 95 % confidence interval.

NPGD
1, 1331–1363, 2014

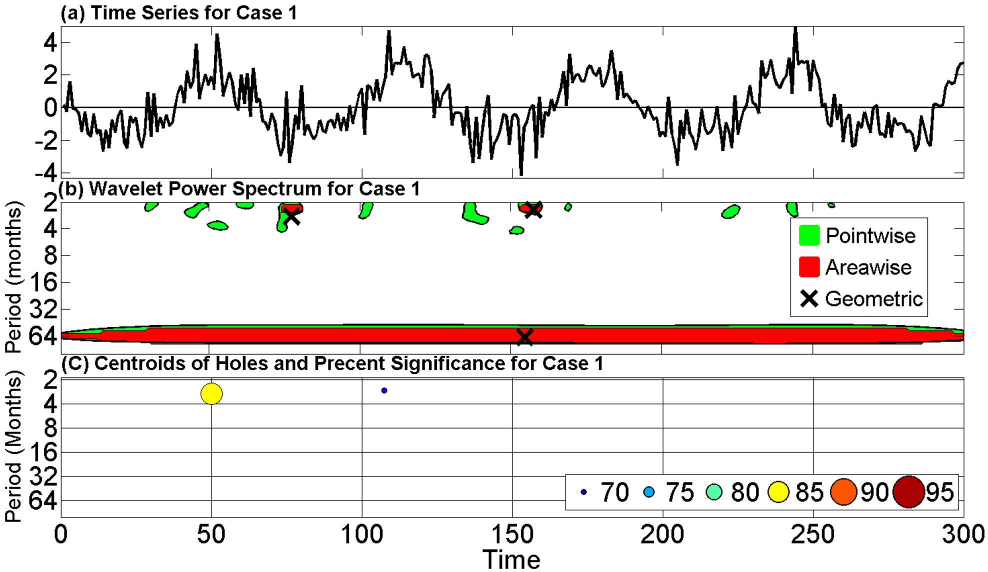

Figure 6. (a) Time series of Case 1, which results from passing a single sinusoidal input with period $\lambda = 64$ through Eq. (16). Gaussian additive white noise with a signal-to-noise of 2 was added to the output response. **(b)** The corresponding normalized wavelet power spectrum. Green shading indicates 95 % pointwise significant patches and red shading indicates 90 % areawise significant subsets. Crosses refer to the centroids of patches whose geometric significance is $\geq$ 90 %. **(c)** Topological wavelet diagram corresponding to the wavelet power spectrum. Points are the centroids of holes at a given pointwise significance level, where both the color and size of the dots indicate the pointwise significance level at which the hole existed.

NPGD

1, 1331–1363, 2014

Geometric and topological approaches to significance testing in wavelet analysis

J. A. Schulte et al.

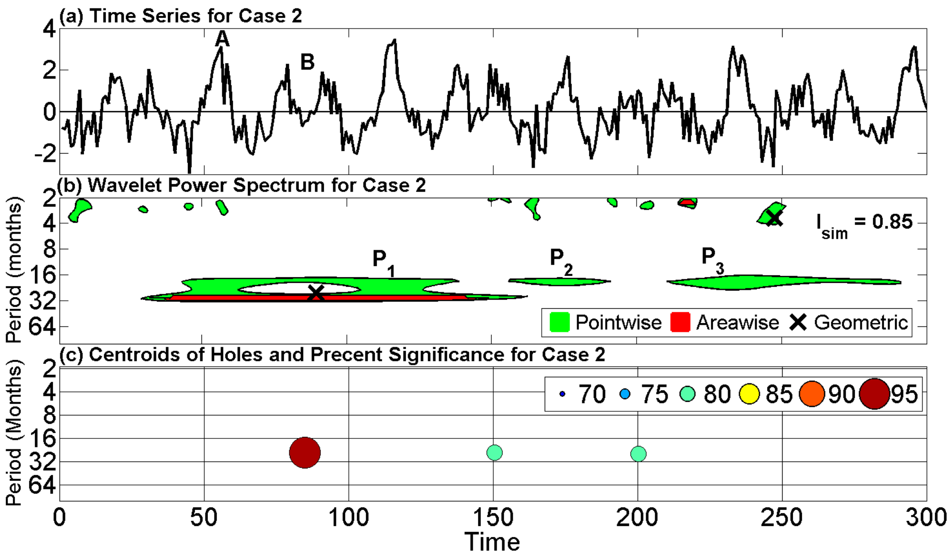

Figure 7. (a) Time series of Case 2. Gaussian additive white noise with a signal-to-noise ratio of 8 was added to the time series. At the point labeled *A* two oscillations resonant, merging two pointwise significance patches in the wavelet domain. At the point labeled *B* no such resonance occurs and the two significance patches separate. **(b)** The corresponding normalized wavelet power spectrum. Features of the wavelet power spectrum are identical to that of Fig. 6. The pointwise significance patch labeled P_1 contains a hole and the pointwise significance patches labeled P_2 and P_3 were falsely deemed insignificant by the geometric and areawise tests. **(c)** Same as Fig. 6c except for the wavelet power spectrum of Case 2.

NPGD
1, 1331–1363, 2014

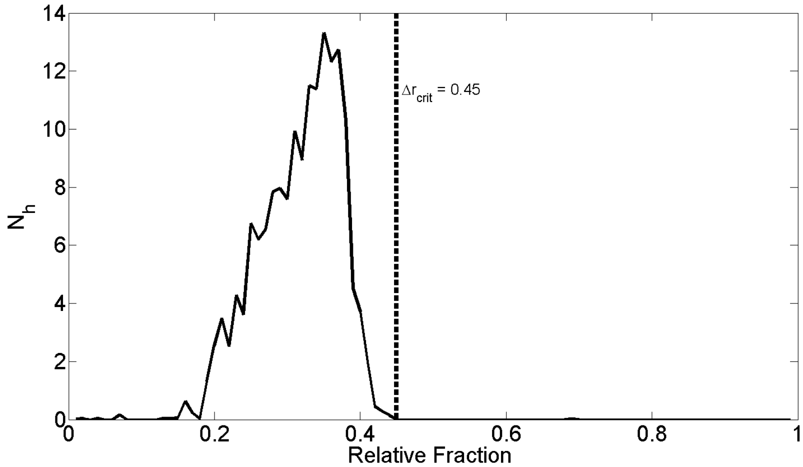

Figure 8. Mean number of holes found in 95 % pointwise significance patches as a function of $\Delta r = (f_2 - f_1)/f_2$ for a sum of two sinusoids with frequency components f_1 and f_2 such that $f_2 > f_1 > 0$. Additive white noise with a signal-to-noise ratio of 30 was added to the sum of sinusoids. Dashed line represents the critical value of Δr, the value beyond which holes will rarely occur between oscillations with frequencies f_1 and f_2.

NPGD
1, 1331–1363, 2014

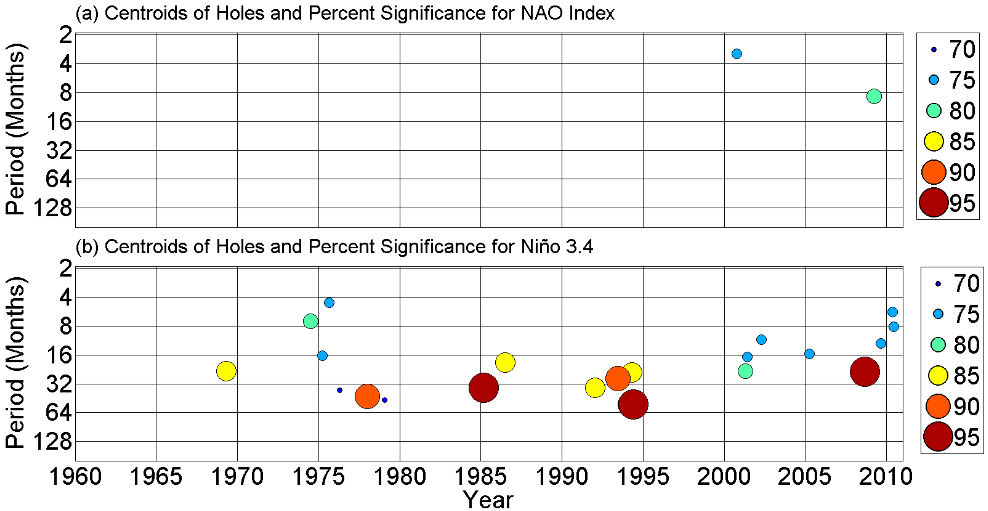

Figure 9. (a) Same as Fig. 6c but for the mean monthly Niño 3.4 index anomalies for 1960–2010. **(b)** Same as Fig. 6c but for the mean monthly NAO index for 1960–2010.

NPGD
1, 1331–1363, 2014

Geometric and topological approaches to significance testing in wavelet analysis

J. A. Schulte et al.

Title Page
Abstract Introduction
Conclusions References
Tables Figures
◀ ▶
Back Close
Full Screen / Esc
Printer-friendly Version
Interactive Discussion